Biomass and Bioenergy 156 (2022) 106315

Contents lists available at ScienceDirect

Biomass and Bioenergy

journal homepage: www.elsevier.com/locate/biombioe

Catalytic conversion of cellulose to levoglucosenone using propylsulfonic acid functionalized SBA-15 and H_2SO_4 in tetrahydrofuran

Oscar Oyola-Rivera [a], Jiayue He [b], George W. Huber [b], James A. Dumesic [b], Nelson Cardona-Martínez [a,*]

[a] Department of Chemical Engineering, University of Puerto Rico, Mayagüez, PR, 00681-9000, Puerto Rico
[b] Department of Chemical and Biological Engineering, University of Wisconsin, Madison, WI, 53706, USA

ARTICLE INFO

Keywords:
Cellulose
levoglucosenone
levoglucosan
SBA-15
propylsulfonic acid

ABSTRACT

The catalytic conversion of cellulose to levoglucosenone (LGO) was studied using dilute sulfuric acid and propylsulfonic acid functionalized SBA-15 (PS-SBA-15) in tetrahydrofuran (THF). We show that the addition of small amounts of a liquid acid catalyst such as sulfuric acid complements the use of a solid acid catalyst for the conversion of cellulose. Sulfuric acid promotes the depolymerization of cellulose into levoglucosan (LGA). The main role of the solid Brønsted acid catalyst is to dehydrate the LGA into LGO. The addition of low concentrations of H_2SO_4 to PS-SBA-15 resulted in an increase in LGO yield of up to 37% (from 18% obtained using an equivalent amount of H_2SO_4 only). Our approach provides a novel alternative for a more environmentally friendly production of LGO.

1. Introduction

Biomass is an abundant renewable carbon source that includes wood, agricultural crops, and agricultural residues [1,2]. Lignocellulose is the main chemical component of these materials [3–7]. Many researchers have studied the acid hydrolysis of cellulose to glucose followed by the dehydration of glucose to produce furans like furfural and 5-hydroxymethylfurfural (HMF) [7–16]. These reactions are usually performed in water. The use of water as a solvent is convenient because it is readily available, has low cost, and is non-toxic. However, its use involves several challenges. The presence of water in the reaction system can compromise the stability of heterogeneous catalysts [17–20]. Water also solvates acidic protons of Brønsted acid catalysts decreasing their activity, this effect can be reduced by replacing water with polar aprotic solvents [21]. In addition, it is hard to control the product selectivity in several of these reactions in the presence of water due to its participation as a reactant. Those factors, and others, have motivated the study of alternative solvents such as renewable biomass derived solvents as reaction medium [7,21–23]. Polar aprotic solvents, like THF, do not have polar hydrogen functional groups (e.g., O–H and N–H) in its structure. The absence of these groups limits the possibility of hydrogen bonding and reaction with some species. These characteristics make polar aprotic solvents convenient media for liquid phase reactions such as cellulose conversion to levoglucosenone.

Levoglucosenone (LGO) is a high value molecule used for the production of solvents, polymers and anti-cancer drugs [7,14,24,25]. It is conventionally produced using the Furacell™ technology developed by Circa™ which involves the catalytic conversion of pine sawdust in sulfolane using phosphoric acid as catalyst in a prototype scale [26]. LGO can be hydrogenated into Cyrene™, a bio-based polar aprotic solvent [26]. Recently, Circa™ announced the construction of a commercial plant in Europe for the production of 1000 tons of Cyrene™ per year from LGO [27].

The first step in the production of LGO from cellulose is the depolymerization of cellulose to levoglucosan (LGA) in the presence of a Brønsted acid catalyst in a polar aprotic solvent [7,14,23]. LGA is then dehydrated to LGO again catalyzed by Brønsted acids [7,23,28]. A generalized reaction pathway for the conversion of cellulose to LGO is shown in Scheme 1.

Alternative routes to produce LGO from cellulosic materials include pyrolysis and liquid phase catalysis using homogenous or heterogeneous catalysts in different solvents [29–31]. Each of these approaches has process and economic advantages and challenges. The catalytic liquid phase route seems to be one of the most attractive due to the lower

* Corresponding author.
E-mail addresses: oscar.oyola@upr.edu (O. Oyola-Rivera), gerryhe@gmail.com (J. He), gwhuber@wisc.edu (G.W. Huber), jdumesic@wisc.edu (J.A. Dumesic), nelson.cardona@upr.edu (N. Cardona-Martínez).

https://doi.org/10.1016/j.biombioe.2021.106315
Received 21 May 2021; Received in revised form 12 November 2021; Accepted 21 November 2021
Available online 26 November 2021
0961-9534/

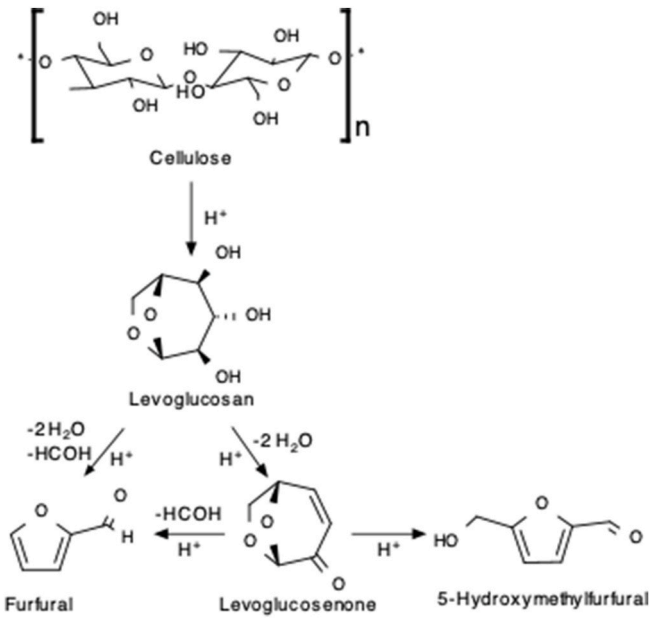

Scheme 1. Generalized reaction pathway for the catalytic dehydration of cellulose to LGO using a Brønsted acid catalyst in the absence of water. MarvinSketch was used for drawing and displaying of chemical structures and reactions, Marvin version 21.3.0, ChemAxon (https://www.chemaxon.com).

temperature required to promote the conversion of cellulosic material to LGO compared to pyrolysis methods [29]. Another advantage is the possibility of improving the separation of LGO if volatile solvents are used, such as tetrahydrofuran (THF) [23].

The liquid phase production of LGO has been studied using liquid and solid acid catalysts. Huber and co-workers studied the conversion of cellulose to LGO using sulfuric acid (H_2SO_4) as a catalyst in polar aprotic solvents [7,23]. They observed LGO yields up to 39.5% from 1 wt% cellulose in THF using H_2SO_4 [23]. Based on a techno economic analysis performed by this group, the cellulose loading needs to be increased to improve the efficiency of this process [23]. The increase in cellulose loading caused a decrease in LGO yields to about 10% [23]. One of the reasons for the decrease in the LGO yield is the hydration of LGA into glucose by the water produced during LGA dehydration to LGO. Oyola-Rivera et al. using a similar approach, but starting with LGA, reported the production of LGO with 59% yield in THF using SBA-15 functionalized with propylsulfonic acid groups (PS-SBA-15) [28]. The surface properties of this catalyst reduced water interactions with the acid sites enhancing the LGO yield [28]. Huang et al. also showed high LGO yields (32%) from LGA using Amberlyst 70 in DMSO and its further improvement to 40% by removing the water produced during the reaction [32]. Those studies demonstrated the potential use of a simple solid Brønsted acid catalyst for the production of LGO at high selectivity and yield in polar aprotic solvents. However, LGA is an expensive molecule to use as a feedstock and it would be highly desirable to produce LGO directly from cellulose. Also, the limited contact between two solid surfaces in a suspension and the accessibility of cellulose into the catalysts pores system restricts the ability of the solid acid catalyst to promote the depolymerization of cellulose.

The objective of this work is to increase the LGO yield from cellulose using the synergistic combination of a solid and a liquid Brønsted acid catalyst. Our goal is to use low concentrations of H_2SO_4 to first maximize the production of LGA from cellulose with a low production of LGO, HMF and furfural. This is followed by the in situ use of PS-SBA-15 for the selective production of LGO from the LGA produced from cellulose depolymerization using H_2SO_4. We studied the use of PS-SBA-15 combined with H_2SO_4 for the dehydration of cellulose to LGO in THF. We show that the use of small amounts of H_2SO_4 is necessary to increase the rate of cellulose depolymerization to LGA. The total LGO yield obtained using PS-SBA-15 in the absence of H_2SO_4 is low (7.1%). However, as we will show in this paper, a combination of sulfuric acid with PS-SBA-15 increases the LGO yield to 37%.

2. Materials and methods

2.1. Materials

Pluronic P123 (Sigma-Aldrich) and tetraethyl orthosilicate (TEOS) (Acros Organics, 98% purity) were used as template and precursor of SiO_2 for PS-SBA-15 synthesis, respectively. Hydrochloric acid (HCl) (Acros Organics, 37% solution in water and Sigma-Aldrich, ACS reagent) was used to dissolve P123 during PS-SBA-15 synthesis. The propyl sulfonic precursor used for the synthesis of PS-SBA-15 was (3-mercaptopropyl)trimethoxysilane (MPTMS) (Alfa Aesar, 95% purity). Hydrogen peroxide solution (H_2O_2) (Fisher Chemical, 30% certified ACS) was used as oxidation agent for the PS-SBA-15 synthesis. Ethanol (Alfa Aesar, 95% purity) was used for the removal of the P123 template. Sulfuric acid (H_2SO_4) (Fisher Chemical, certified ACS plus) was used as a catalyst and for catalyst treatments. Tetrahydrofuran (THF) (Sigma-Aldrich, anhydrous, inhibitors-free, 99.9% purity and Acros, anhydrous, 99.9% stabilized with BHT) was used as a solvent for reactions and catalysts treatments. Helium (He) (Praxair, 99.999% and Airgas, 99.999%) was used to pressurize the reactor. Cellulose (Acros Organics, average particle size 50 μm) was used as reactant. Levoglucosan (LGA) (Acros Organics, 99% purity and CarboSynth, purity 98%) was used as a reactant and standard. Levoglucosenone (LGO) (GlycoSyn 90% purity and Apollo Scientific, 98% purity), 5-hydroxymethilfurfural (HMF) (Acros Organics, 98% purity and Sigma-Aldrich, 99% purity) and furfural (Acros Organics, 99% purity) were used as standards. 1-butanol (Fisher Chemical, certified ACS) was used as an internal standard for GC-FID analyzes. Sodium chloride (NaCl) (Fisher Chemical, certified ACS) and sodium hydroxide (NaOH) (Acros Organics, 98.5% purity) were used for the determination of PS-SBA-15 acid concentration.

2.2. Catalyst preparation

We used SBA-15 as the support for propylsulfonic acid. SBA-15 is an ordered mesoporous silica used in many catalytic applications due to its high surface area and simple preparation [33]. The synthesis of propylsulfonic-functionalized SBA-15 was performed using the synthesis procedure reported by Stucky and co-workers [34]. The first step of this synthesis was to dissolve 15 g of P123 in 480 mL of 2 M HCl and 24 mL of DI water at 313 K. Afterwards, 25 mL of TEOS were added and aged for 45 min at 313 K under stirring. Then MPTMS and 30 wt% H_2O_2 solution were added to the mixture. The mixture was aged for 20 h at 313 K under stirring. Once the aging at 313 K was completed, the temperature was increased to 373 K and aged for an additional 20 h. The solid precipitate was filtered and washed with water. Afterwards, the P123 template was removed by refluxing ethanol for 24 h. After removing the copolymer template, the solid was filtered and washed with ethanol. Finally, the PS-SBA-15 was dried under vacuum at 353 K. The structure of the propylsulfonic acid group on the surface of SBA-15 is reported elsewhere [35].

2.3. Catalyst characterization

An accelerated surface area and porosimetry system Micromeritics ASAP 2020 unit was used to determine the BET surface area using nitrogen physisorption isotherms at 77 K. The α_s-plot method was used to determine the micro and mesopore volumes [36–38]. A pore size distribution (PSD) analysis including the correction of the Kruk-Jaroniec-Sayari (KJS) for the statistical film thickness in the Barret-Joyner-Halenda (BJH) method was used to determine the mesopore diameter [39]. Before the N_2 physisorption experiments, the

catalysts were degassed at 423 K under a vacuum of 0.01 bar for 4 h.

The powder X-ray diffraction (XRD) patterns were obtained using a Bruker D8 Discover X-Ray diffractometer equipped with cross beam optics and a Cu K_α target, operating at 50 kV and 1000 μA using small angle mode.

The acid loading of the PS-SBA-15 was determined by ion exchange of 0.10 g of the catalysts with 20 mL of an aqueous solution of 2 M NaCl for 2 h and titrated with an aqueous solution of 0.01 M NaOH.

2.4. Catalytic performance

The conversion of cellulose was studied using high-pressure 100 mL batch reactors from Parr Instruments (model 4793 and 4560). The model 4560 has the capability to remove samples during the reaction. This reactor was used to evaluate the effect of time on the cellulose conversion. The heating of the reactor was achieved using a rigid heating mantle controlled with a close loop temperature controller, model 4838 or 4848 from Parr Instruments. The temperature was measured using an Omega JQSS-M30G-300 Type J thermocouple of 1/8 in diameter. The reactor, cellulose and catalyst were previously dried at 373 K overnight. The catalytic performance experiments were performed for three different cellulose loadings of 0.54 g, 2.70 g and 5.93 g to reach 1 wt%, 5 wt% and 10 wt%, respectively. The solid acid catalyst loading was varied from 88 to 100 mg. In a typical experiment, the desired amount of cellulose and solid catalyst, previously dried, were added to the reactor followed by the addition of 60 mL of THF and 1–64 μL of sulfuric acid to reach from 0.3 to 20 mM H_2SO_4. Then, the reactor was closed and purged with He five times. The reactor was pressurized with He to 34 bar and heated to the desired temperature and re-pressurized with He to 69 bar. The stirring rate was maintained at 600 rpm. Time equal zero was set to the point when the temperature reached the desired set point. For single point runs the reactor was quenched after 30 min of reaction in an ice-water bath. For the experiments as a function of reaction time, time equal zero was set to the point when heating was started. After 40 min of heating the reactor reaches the temperature set point of 483 K. After the reaction time was completed the reactor was quenched in an ice water bath. The resulting reaction liquid mixture was removed from the reactor and the residual solid was filtered, washed with DI water and dried at 373 K overnight. A sample of 5 mL of the liquid reaction mixture was mixed with 10 μL of 1-butanol and analyzed using GC. 1-Butanol was used as internal standard. For the runs performed to evaluate the effect of time, a sample was taken from the reactor periodically, quenched in a dry ice bath and analyzed using HPLC.

2.5. Thermal stability tests

The thermal stability of propyl sulfonic acid functionalized SBA-15 in 1.2 mM H_2SO_4 in THF was studied by treating the catalyst sample at 483 K and 69 bar in THF in one of the batch reactor systems described above. The samples were treated for 40, 70 and 100 min. The solid was filtered and washed with THF to remove any physisorbed species and dried at 353 K under vacuum overnight. Finally, the solid was characterized using XRD, BET and acid-base titration to determine changes in the physicochemical properties of the catalyst.

2.6. Analytical methods

The cellulose conversion products analyses were performed using an HP5890 gas chromatography (GC) system equipped with a flame ionization detector (FID) and a J&W HP-5MS capillary column. Helium was used as the carrier gas with a constant flow of 0.4 ml/min. The injector port and the detector temperatures were maintained at 513 K and 523 K, respectively. The GC oven temperature was kept at 313 K for 3 min, and then the temperature was increased to 513 K using a heating ramp of 7.5 K/min and held 513 K for 15 min. The sample injection volume was 1 μL.

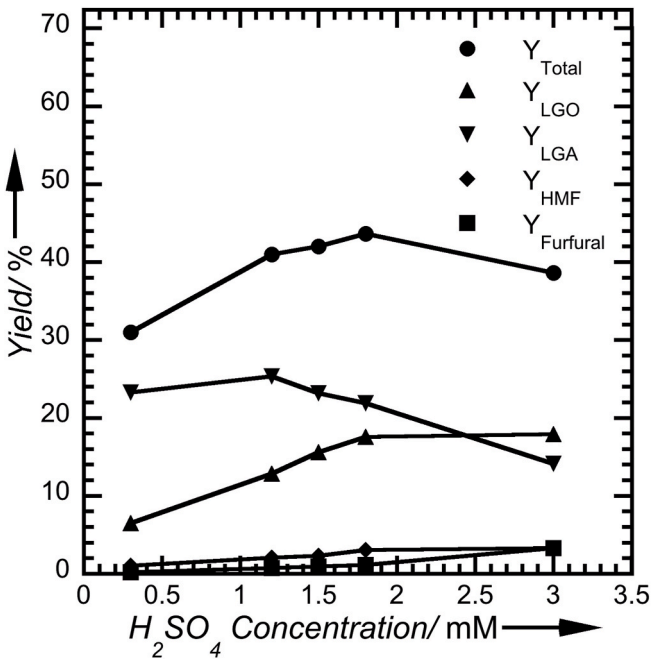

Fig. 1. Effect of H_2SO_4 concentration on product yields for 1 wt% cellulose conversion in THF at 483 K and 69 bar He after 30 min of reaction.

Table 1
Physicochemical properties of PS-SBA-15 before and after treatment with 1.2 mM H_2SO_4 in THF at 483 K.

Time (min)	C_{H+} [a] (mmol/g)	S_{BET} [b] (m^2/g)	S_{Ext} [c] (m^2/g)	D_p [d] (nm)	$V_{P/Po=0.99}$ [e] (cm^3/g)	V_p [f] (cm^3/g)	V_m [g] (cm^3/g)
0	0.96	734	26	5.8	0.63	0.59	0.00
40	0.87	511	8	6.2	0.43	0.39	0.03
70	0.79	911	33	6.2	0.80	0.71	0.02
100	0.73	550	24	6.2	0.48	0.43	0.01

[a] H^+ loading on PS-SBA-15 determined by ion-exchange and titration.
[b] BET surface area.
[c] External surface area.
[d] Average mesopore diameter.
[e] Total pore volume determined at a relative pressure of 0.99.
[f] Total mesopore volume.
[g] Total micropore volume.

The samples taken during the reaction for the evaluation of the effect of reaction time were analyzed using a high performance liquid chromatograph (Shimadzu LC-20AC) equipped with a refractive index (Shimadzu RID-10A) used for LGA analysis and a UV (Shimadzu UV–vis SPD-20AV) used for the analysis of LGA, HMF and furfural. A Bio-Rad Aminex HPX-87H column was used for the separation of the reaction products. The mobile phase was an aqueous solution of 5 mM H_2SO_4 with a flow rate of 0.6 mL/min. The column temperature was held at 303 K. The sample injection volume was 1 μL.

The carbon yield for each product was calculated as the ratio of the determined moles of carbon of product and the initial carbon moles. The total carbon yield was calculated as the ratio of the sum of the moles of carbon determined for each product and the initial carbon loading. The turn over frequencies (TOF) for the species produced were calculated based on the acidic proton loading.

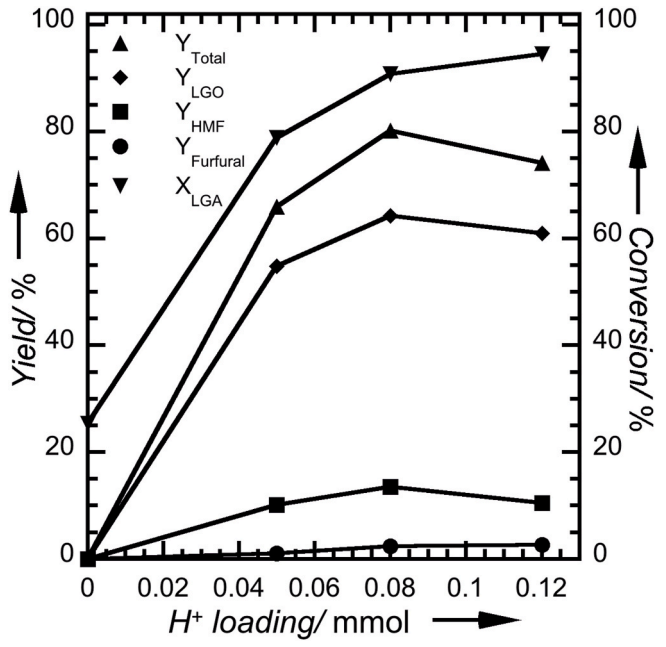

Fig. 2. Effect of protons loading using PS-SBA-15 on LGA conversion using 14.3 mM LGA in THF at 483 K and 69 bar He for 30 min reaction.

3. Results and discussion

3.1. Catalytic performance

3.1.1. Effect of H_2SO_4 concentrations on cellulose dehydration

We evaluated the use of H_2SO_4 as catalyst for the production of LGA and LGO from cellulose in THF for the dehydration of 1 wt% cellulose loading at 483 K for 30 min, as shown in Fig. 1. We observed LGA, LGO, HMF and furfural as products. LGA was the most abundant product for acid concentrations between 0.3 and 1.8 mM H_2SO_4. Treating cellulose in THF without catalyst produced a trace amount of LGA with no other soluble products detected. These observations suggest that the depolymerization of cellulose without the addition of a liquid acid is low or negligible at the reaction conditions used in Fig. 1 and H_2SO_4 is required for cellulose depolymerization to LGA. Increasing the H_2SO_4 concentration causes a decrease in the LGA yield while the LGO increases by dehydration of LGA to LGO [7,23]. The HMF yield also rises with increasing acid concentration which is likely due to isomerization of LGO to HMF [40]. Increasing the H_2SO_4 concentration from 1.8 to 3.0 mM causes a decrease in LGA yields from 21.9% to 14.1%, making LGO the most abundant product. However, the LGO yield remains constant and the furfural yield increases from 1.1% to 3.3%. Increasing the concentration of H_2SO_4 to 3 mM leads to degradation products such as humins and furfural.

Based on these results we used a H_2SO_4 concentration of 1.2 mM in combination with a solid acid catalyst for the production of LGO from cellulose in other experiments in this paper. At this H_2SO_4 concentration the production of LGA is higher than the production of LGO, HMF and furfural. Also, at this concentration we observed the highest LGA yield.

3.1.2. Effect of solid Brønsted acid loading on LGA dehydration

We studied the effect of the propylsulfonic acid concentration on the PS-SBA-15 catalyst on the conversion of LGA to LGO to find the concentration of propylsulfonic acid needed that maximizes the production of LGO. Fig. 2 shows the effect of changing the acid content using propyl sulfonic acid functionalized SBA-15 on the production of LGO from LGA in THF at 483 K. In these experiments we used the amount of LGA produced from cellulose in the run using 1.2 mM H_2SO_4 and 1 wt% cellulose loading. We prepared catalysts with different contents of propyl sulfonic acid groups to vary the loading of Brønsted acid sites. For the reaction that had 0.12 mmol H^+ loading we used a higher mass (100 mg) of the catalyst with 0.96 mmol H^+/g. In the absence of a catalyst we observed an LGA conversion of 25% with no detectable products in the liquid phase. We observed the production of a dark brown solid suggesting the formation of degradation products such as humins. In the presence of the solid acid catalyst we observed the production of LGO, HMF and furfural. The main product from the LGA dehydration using PS-SBA-15 catalysts is LGO with yields from 55% to 64%. The other products detected were HMF and furfural with yields from 10% to 13% and 1–3%, respectively. The conversion of LGA rises by increasing the acid loading. Yet, the LGO and HMF yields pass through maxima at an acid loading of 0.08 mmol H^+. The furfural yield continued to increase with increasing acid loading. Based on these observations we decided to use 88 mg of PS-SBA-15 with a propylsulfonic acid loading of 0.96 mmol/g for the conversion of LGA produced from cellulose by H_2SO_4 in the same system to target 0.08 mmol H^+ from PS-SAB-15 in the reactor. Using this amount of solid acid catalyst we obtained the highest total carbon yield (80%) at an LGA conversion of 91%.

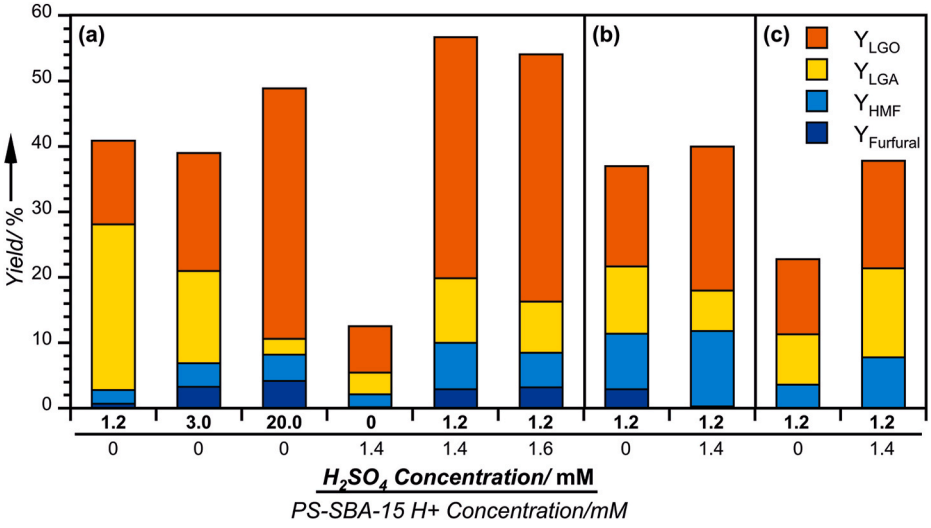

Fig. 3. Cellulose conversion at 30 min of reaction for (a) 1 wt%, (b) 5 wt% and (c) 10 wt% cellulose loadings using H_2SO_4 and PS-SBA-15 in THF at 483 K and 69 bar He.

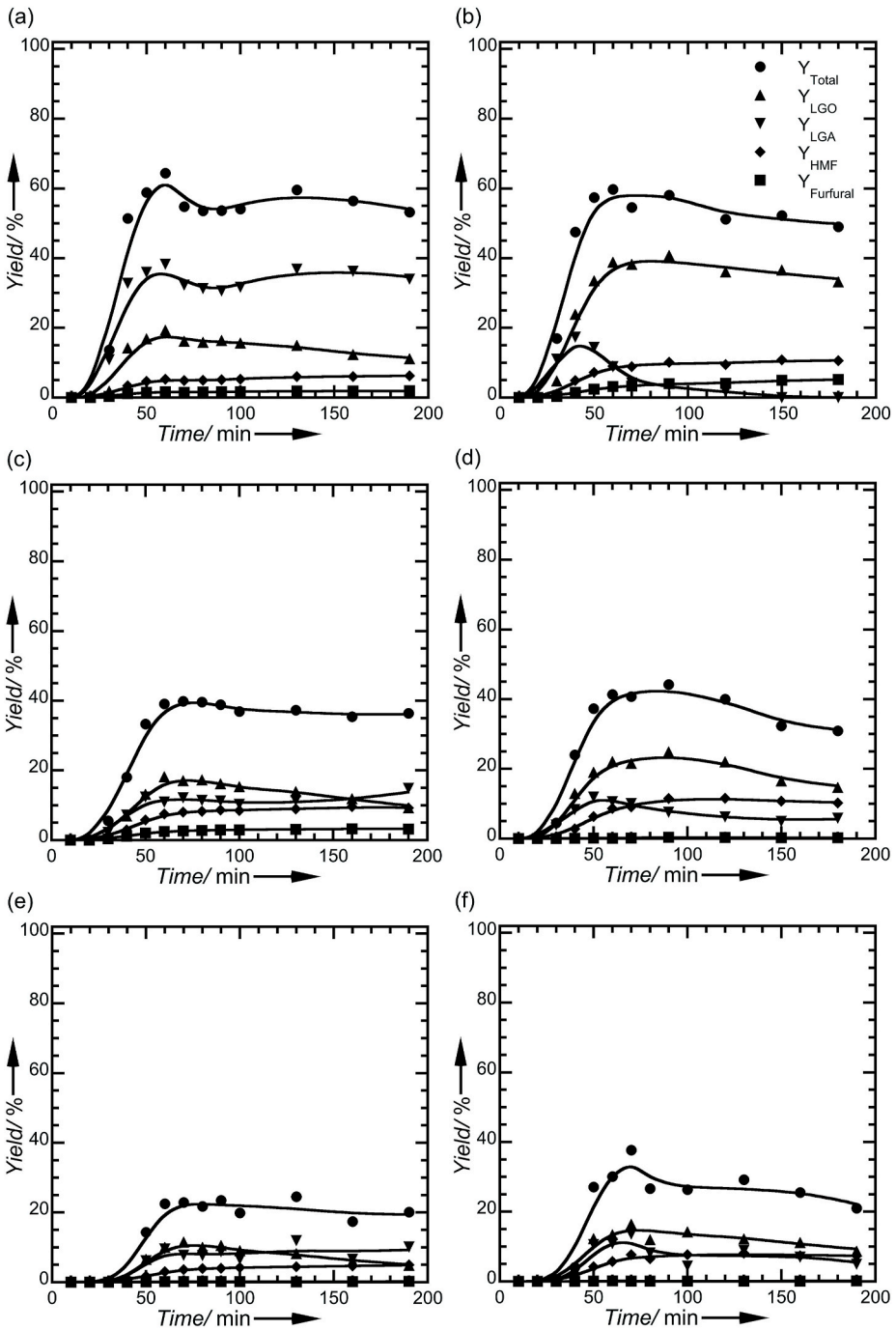

Fig. 4. Cellulose conversion as a function of reaction time for (a, b) 1 wt%, (c, d) 5 wt% and (e, f) 10 wt% cellulose loadings using 1.2 mM H_2SO_4 (a, c, and e) and a combination of 1.2 mM H_2SO_4 and 88 mg (1.4 mM H^+) PS-SBA-15 (b, d, and f) in THF at 483 K and 69 bar He.

3.1.3. Effect of solid Brønsted acid catalyst on cellulose dehydration

The synergistic effect of H_2SO_4 and PS-SBA-15 on the conversion of cellulose in THF is shown in Fig. 3 along with the LGO, LGA, HMF, and furfural yields for 1, 5 and 10 wt% cellulose dehydration at 483 K. Fig. 3a shows the results for 1 wt% cellulose. When cellulose was dehydrated using PS-SBA-15 in the absence of H_2SO_4 the total carbon yield was 13% and the most abundant product observed was LGO with a yield of 7%. The mesopore diameter of PS-SBA-15 is 5.8 nm and the average particle size of the cellulose used in this study is around 50,000 nm. Cellulose with this particle size cannot enter the pores of the catalyst. We believe that the solid acid catalyst loses part of the sulfonic acid groups during the reaction that go to the bulk of the solvent and act as a liquid acid catalyst promoting the depolymerization of cellulose to LGA and its eventual conversion to LGO. The partial leaching of the acid sites from PS-SBA-15 was confirmed under the reaction conditions and will be discussed later in this article. The loss of acid sites from PS-SBA-15 at the reaction conditions studied in this section was 9%. The conversion of 1 wt% cellulose was also studied using 1.2 mM H_2SO_4 in the absence of PS-SBA-15. The results show that the cellulose is preferentially converted to LGA with a yield of 25%, suggesting that at this H_2SO_4 concentration the main reaction route is the depolymerization of cellulose as discussed above. Combining H_2SO_4 and PS-SBA-15 the total carbon yield increases to 57%. The most abundant product observed was LGO with a yield of 37%. The LGA yield was 10%. The LGA yield decreases with increasing the concentration of either the liquid or solid catalyst. The LGO yield is 37% using both catalysts compared to 13% using only

H_2SO_4 at a concentration of 1.2 mM. These observations suggest that the main role of H_2SO_4 is cellulose depolymerization to LGA and that PS-SBA-15 is more effective at converting LGA to LGO than H_2SO_4. This result is consistent with our previous finding [28]. The HMF and furfural yields are similar when using H_2SO_4 or PS-SBA-15 on their own. Thus, it is difficult to distinguish if one of the two catalysts is mainly responsible for the production of HMF and furfural.

We studied the conversion of 1 wt% cellulose using 20 mM H_2SO_4 in the absence of PS-SBA-15 at 483 K in THF to understand the effect of addition of the solid acid catalyst at higher H_2SO_4 concentration. The total carbon yield (49%) was lower using 20 mM H_2SO_4 in the absence of PS-SBA-15, while the LGO yield (38%) was almost the same to that obtained using 1.2 mM H_2SO_4 and PS-SBA-15 (37%). The main difference was in the amount of LGA and HMF produced, which was higher using 1.2 mM H_2SO_4 and PS-SBA-15. The total acid proton loading using 1.2 mM H_2SO_4 and 88 mg (1.4 mM H^+) PS-SBA-15 is equivalent to 2.6 mM H_2SO_4. That concentration corresponds to 13% of the acid proton loading using 20 mM H_2SO_4. However, the LGO yield is about the same for 20 mM H_2SO_4 as for the 1.2 mM H_2SO_4 with the PS-SBA-15 catalyst suggesting that PS-SBA-15 is more active than H_2SO_4 for the conversion of LGA to LGO The same conclusion is obtained by comparing the results for 3 mM H_2SO_4 with those using 1.2 mM H_2SO_4 and 88 mg (1.4 mM H^+) PS-SBA-15 (equivalent to 2.6 mM H_2SO_4) shown in Fig. 3a. Using PS-SBA-15 produces 2.1 times more LGO (37%) than using an equivalent amount of H_2SO_4 (18%). This is related to differences in activity of H_2SO_4 and PS-SBA-15 for the conversion of LGA. We previously reported the turn over frequency (TOF) for LGA conversion using H_2SO_4 or PS-SBA-15 at the same reaction conditions shown here. The TOF for the consumption of LGA using H_2SO_4 was 0.7 ks^{-1} while for PS-SBA-15 was 2.3 ks^{-1} [28]. These differences in activity were related to the reduction of the interaction of water produced during the reaction with the acid sites of PS-SBA-15 by the presence of a high concentration of hydroxyl groups on SBA-15 [28]. Water can promote the solvation of the acid proton causing the stabilization of the proton and reducing its activity [21]. Since PS-SBA-15 is more active for the conversion of LGA to LGO than H_2SO_4, adding PS-SBA-15, instead of increasing the concentration of H_2SO_4, improves the LGO yields from cellulose. The total carbon yield increases 1.5 times using 1.2 mM H_2SO_4 and 88 mg (1.4 mM H^+) PS-SBA-15 (57%) compared to 3 mM H_2SO_4 (39%). Suggesting that PS-SBA-15 not only improves the rate of LGO formation, but also has a synergistic effect with H_2SO_4 to increase the rate of cellulose conversion.

The conversion of 1 wt% cellulose was also studied using 1.2 mM H_2SO_4 at different loadings of PS-SBA-15. The total carbon yield at 1.6 mM H^+ from PS-SBA-15 was 54%, which is lower than that obtained using 1.2 mM H_2SO_4 and 1.4 mM H^+ from PS-SBA-15. However, the yields towards LGO (38%) and furfural (3%) were slightly higher. On the other hand, the yield for LGA (8%) and HMF (5%) were lower.

Fig. 3b and c shows the carbon yields for LGA, LGO, HMF, and furfural obtained for the conversion of 5 and 10 wt% cellulose in THF at 483 K using H_2SO_4 and PS-SBA-15. The LGA yield decreases as the cellulose loading increases when only H_2SO_4 was used as a catalyst. The LGO, HMF and furfural yields increase when the cellulose loading was increased from 1 to 5 wt%. All identifiable products yields then decrease by increasing the cellulose loading from 5 to 10 wt%. Combining H_2SO_4 and PS-SBA-15 for the conversion of 5 and 10 wt% cellulose loading increases the total carbon and LGO yields compared to those obtained using only H_2SO_4, at 1 wt% cellulose loading. These results confirm that the addition of PS-SBA-15 improves the conversion of cellulose to LGO. The results suggest that the rate of LGO degradation to humins is higher at 5 wt% than at 1 wt% cellulose. Increasing the cellulose loading from 5 to 10 wt% causes an increase in the LGA yield while the LGO and HMF yields decrease. Despite the fact that the yields decrease by increasing the cellulose loading, the concentrations of LGA, LGO and HMF produced increase as the cellulose loading increases. Increasing the production of LGO also causes an increase in the amount of water produced. Hence, at 10 wt% cellulose the water concentration appears sufficiently high to cause a reduction in the catalytic activity of the acid protons, reducing its performance to produce LGO and its conversion to HMF. The activity of the acid protons is reduced by its solvation and stabilization in the presence of water, as described by Mellmer et al. [21].

To assess the sustainability of our process we estimated the Reaction Mass Efficiency (RME) [41,42] and Environmental Factor (E-factor) [43] and compared it with the values for the current commercial process for the production of LGO that uses phosphoric acid (H_3PO_4) and sulfolane [26,44,45] and with the process proposed by Huber et al. using sulfuric acid (H_2SO_4) in tetrahydrofuran (THF) [23]. Our calculations are included in Appendix A and the results are summarized in Table A1. The Reaction Mass Efficiency for the conversion of 1 wt% cellulose using H_2SO_4 as described by Huber [23] and the combination of 88 mg (1.4 mM H^+) PS-SBA-15 and 1.2 mM H_2SO_4 proposed in this work are more than two times higher than the RME for the FuraCell™ process. However, the E-factor is slightly higher due to the amount of solvent used and its recovery, but it is still inside the E-factor range for the fine chemical industry (5–50) [43]. The E-factor improves when we increase the cellulose loading. For a loading of 5 wt% the E-factor for our process is 64% of the value for the FuraCell™ process and decreases further to 52% when we increase the cellulose loading to 10 wt%. On the other hand, the RME decreases as the cellulose loading increases, but at the highest cellulose loading used in this work the RME is still higher than the RME estimated for the FuraCell™ process. Based on these results we suggest that the use of PS-SBA-15 and H_2SO_4 in THF for the conversion of cellulose to LGO can be an alternative process for the production of LGO at higher mass yields and lower ratio of waste to product. In addition, the concentration of acid used in our process is about 200 times lower than that used in the FuraCell™ process, reducing corrosive hazards during the production of LGO from cellulose.

3.1.4. *Effect of reaction time on cellulose dehydration*

Fig. 4 shows the carbon yields as a function of reaction time for the conversion of 1, 5 and 10 wt% cellulose at 483 K in THF using H_2SO_4 and PS-SBA-15. Time zero was defined as the moment at which the heating started. The heat up time to reach 483 K was 40 min. The maximum total carbon yield of identifiable products was obtained at 60–70 min of reaction times for all of these experiments. The addition of PS-SBA-15 does not cause an increase in the total carbon yield of identifiable products compared to those obtained using only H_2SO_4, as shown in Fig. 4. The distribution of products does change when PS-SBA-15 is added. The most abundant product during the conversion of 1 wt% cellulose loading using H_2SO_4 was LGA, as shown in Fig. 4a. The addition of PS-SBA-15 causes an increase in the LGO yield suggesting that the PS-SBA-15 has the main role in the conversion of LGA, while H_2SO_4 is the main responsible for the depolymerization of cellulose to LGA. A similar behavior is also observed for the conversion of 5 and 10 wt% cellulose.

The total carbon, LGA and LGO yields decrease as the cellulose loading increases. The yield of LGA decreases while the production of LGO increases by the addition of PS-SBA-15. The LGA yield passes through a maximum at 40 min of reaction and no LGA was observed after 150 min of reaction during the conversion of 1 wt% cellulose using PS-SBA-15, as shown in Fig. 4b. The time to reach the maximum LGA yield increases at high cellulose loadings. The maximum LGA yield was obtained at 50 and 70 min for 5 and 10 wt% cellulose, respectively (Fig. 4d and f). This behavior can be attributed to an increase in the cellulose to catalysts ratio as the cellulose loading increases. The time to reach the maximum LGO yield was 90 min starting with 1 and 5 wt% cellulose loading. It decreases to 70 min when the cellulose loading was increased to 10 wt%.

LGA was completely consumed with a 1 wt% cellulose feed, while the LGA yield reached a plateau for the 5 and 10 wt% cellulose feeds. As mentioned above, the concentration of LGO produced increases as the cellulose loading increases. For every 1 molecule of LGO produced, 2 molecules of water are produced. This causes a rise in the concentration of water during the reaction. The production of water is higher at

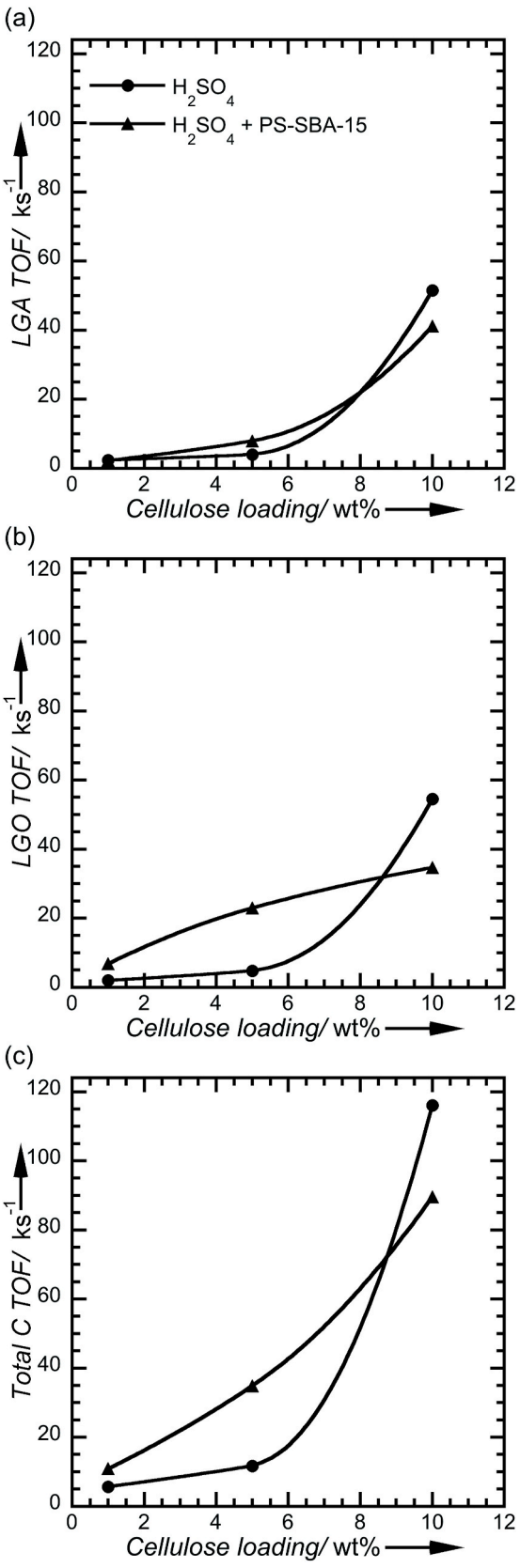

Fig. 5. Average TOF for the production of (a) LGA, (b) LGO and (c) total products using only 1.2 mM H_2SO_4 and a combination of 1.2 mM H_2SO_4 and 88 mg (1.4 mM H^+) PS-SBA-15 at 483 K in THF.

cellulose loadings of 5 and 10 wt% than for a cellulose loading of 1 wt%. In a previous study, we observed that the catalytic activity of H_2SO_4 and propylsulfonic acid functionalized SiO_2 catalysts decrease as the production of water increases by increasing the concentration of LGA as the reactant [28]. Based on these observations we believe that the increase in the amount of water produced caused by increasing the cellulose loading is sufficiently high to reduce the activity of the acid sites effectively stopping the catalytic conversion of LGA.

Fig. 5 shows the TOF based on the total loading of H^+ for the production of LGA and LGO using H_2SO_4 and PS-SBA-15 at 483 K in THF. The TOF for the production of LGA, LGO and the total detectable liquid products increases by increasing the cellulose loading. The TOF for the production of LGA is almost the same with and without using PS-SBA-15. This supports our theory that the cellulose depolymerization is mainly promoted by H_2SO_4 and the presence of PS-SBA-15 does not contribute significantly to the depolymerization of cellulose. The TOF for LGO production is higher than the TOF for LGA at cellulose loadings of 1 and 5 wt%. Increasing the cellulose loading to 10 wt% causes an increase in both rates, but at this loading the TOF for the production of LGA is higher than that for LGO. This suggests that at high cellulose loadings the cellulose depolymerization rate is higher than the LGA dehydration rate at these reaction conditions or to a reduction in catalyst activity due to an increase in the water concentration. At 10 wt% cellulose loading the TOFs are higher when only H_2SO_4 is used as catalyst. However, the production of LGO is higher using the combination of PS-SBA-15 and H_2SO_4 as catalysts. The amount of water produced is also higher, suggesting that the difference in the TOFs obtained with the combination of PS-BSA-15 and H_2SO_4 are related to a decrease in the catalytic activity due to the increase in the concentration of water.

3.2. PS-SBA-15 thermal stability in THF

SBA-15 and acid functionalized SBA-15 are not stable at temperatures higher than 473 K in water [17,46,47]. We also observed that the physicochemical properties of PS-SBA-15 change in THF at 483 K in the absence of H_2SO_4 [28]. For those reasons, we evaluated the thermal stability of PS-SBA-15 in THF with 1.2 mM H_2SO_4 at 483 K for different treatment times. Table 1 shows the physicochemical properties for untreated and treated PS-SBA-15 with 1.2 mM H_2SO_4 in THF at 483 K. The catalyst was treated at the following conditions in this mixture: heating the reactor from 303 to 483 K for 40 min (40 min), holding at 483 K for 30 min after the 40 min ramp (70 min) and holding at 483 K for 60 min after the 40 min ramp (100 min). The acid concentration of the PS-SBA-15 decreases with increasing treatment time. After 70 min the catalyst loses around 18% of the acidity. From our previous work, we observed that treating the catalyst in THF without H_2SO_4 causes a decrease in the acidity of around 16% after 70 min of treatment [28]. We also observed that the acid sites concentration in PS-SBA-15 remained the same by increasing the treatment time in the absence of H_2SO_4 [28]. Here, we observed that the loss of acidity as the treatment time increase is linear at our reaction conditions. The presence of H_2SO_4 causes an increase in the loss of the acid functionalization of PS-SBA-15.

The BET surface area decreases after 40 min of treatment, then increases after 70 min of treatment and again falls after 100 min. This behavior was also observed for the external surface area, total and mesopore volumes. However, the micropores volume increases after 40 min treatment and then decreases after 70 and 100 min treatments. The average pore diameter increases after 40 min treatment and remains the same after 70 and 100 min treatments. We previously reported a similar behavior by treating PS-SBA-15 under the same conditions in THF without H_2SO_4 [28]. This was attributed to the loss of silica from PS-SBA-15 at these conditions in THF since the surface areas and pores volumes were changing, but the ordered porous structure was not changing based on XRD data [28]. Since the changes in surface areas and pore volumes were observed in the presence and absence of H_2SO_4 it is difficult to determine with this data the effect of H_2SO_4 on the textural

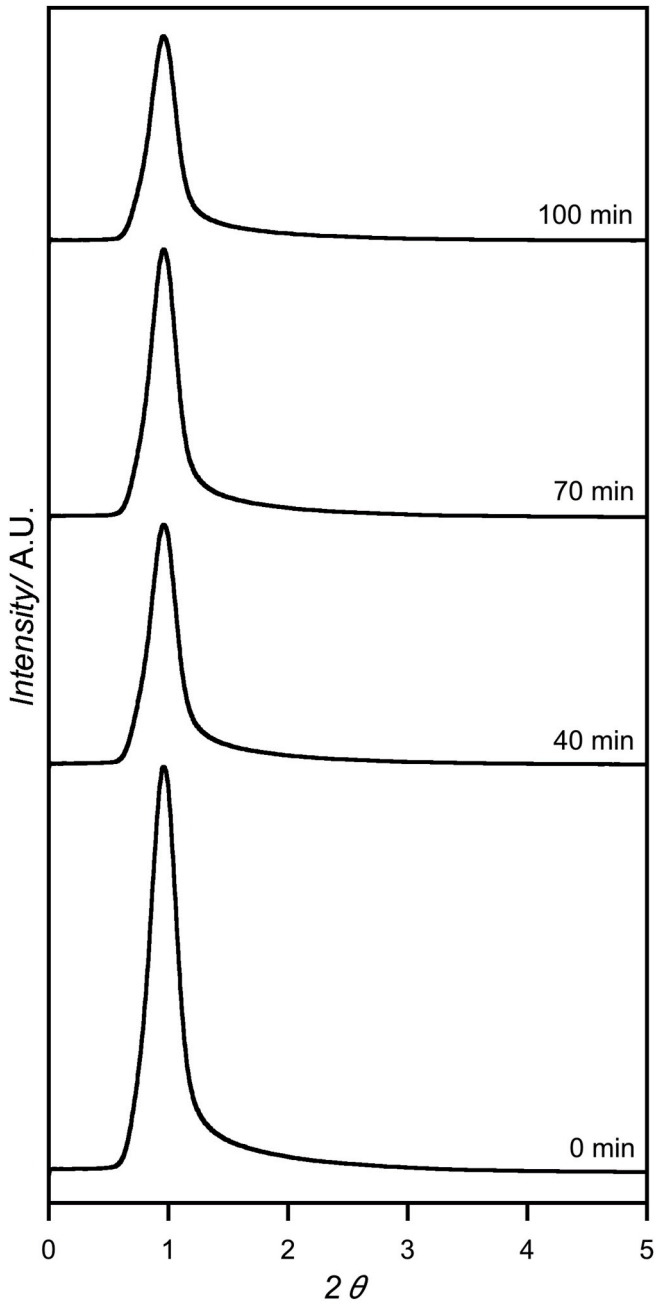

Fig. 6. Powder XRD pattern for PS-SBA-15 after thermal treatments for different times using 1.2 mM H_2SO_4 in THF at 483 K.

properties of PS-SBA-15. Therefore, in both cases we believe that the changes in the textural properties of the catalyst are related to a loss and a re-arrangement of silica in the SBA-15 walls due to its exposure to THF at 483 K.

Figs. 6 and 7 show the small angle XRD patterns and the N_2 adsorption-desorption isotherms for PS-SBA-15 after treatment with 1.2 mM H_2SO_4 in THF at 483 K, respectively. The (100) peak corresponding to the hexagonal arrangement of the mesopores in SBA-15 remains after treating the sample, as shown in Fig. 6. The N_2 adsorption-desorption isotherms for treated PS-SBA-15 preserves a type IV shape. These results suggest that the hexagonal mesopore arrangement of the SBA-15 is not completely lost by the physicochemical changes discussed above. This supports the hypothesis that SBA-15 may be losing silica under these conditions.

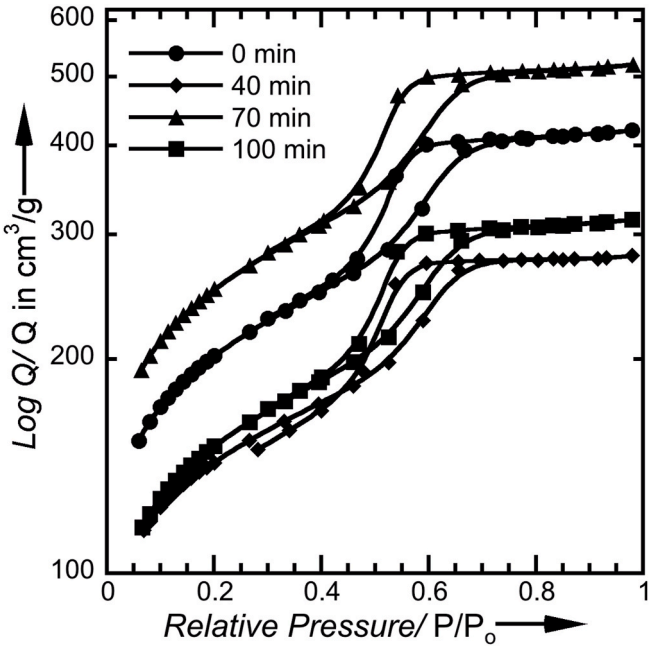

Fig. 7. Nitrogen adsorption-desorption isotherms for PS-SBA-15 after thermal treatments for different times using 1.2 mM H_2SO_4 in THF at 483 K.

4. Conclusions

The catalytic conversion of cellulose in the presence of a Brønsted solid acid was studied using PS-SBA-15 in THF. It was shown that it is necessary to use a liquid acid catalyst at low concentrations to obtain sufficient depolymerization of cellulose to LGA. The conversion of cellulose to LGO consists of two main steps. The first step is the depolymerization of cellulose to LGA promoted mainly by H_2SO_4 followed by the dehydration of LGA to LGO promoted mainly by PS-SBA-15. The use of low concentrations of H_2SO_4 and PS-SBA-15 combined for the conversion of cellulose to LGO results in an increase of the LGO and total carbon yields of over 2.1 times for LGO and 1.5 times for total carbon compared to that obtained using an equivalent amount of H_2SO_4 only. This can be attributed to the higher activity of PS-SBA-15 to convert LGA to LGO compared to H_2SO_4. Increasing the cellulose loading to 10 wt% causes an increase in the water concentration causing a reduction of the catalytic activity of the acid proton affecting the production of LGO. The physicochemical properties of the solid acid catalysts change after treatment with 1.2 mM H_2SO_4 in THF, the most relevant change is the partial leaching of acid sites at the reaction conditions. The leached acid sites can act as liquid catalysts, however this contribution is low based on the results for cellulose conversion using only PS-SBA-15. The results obtained in this study show that the synergistic combination of PS-SBA-15 and H_2SO_4 catalysts at low acid loading improves the LGO production from cellulose compared to the use of H_2SO_4 only.

Acknowledgements

This work was supported by the National Science Foundation (N.C. M. and O.O.R.) [grant numbers HRD-1345156 and OIA-1632824]; and the Department of Energy (J.H., G.W.H and J.A.D.) [grant number DE-EE0006878]. The funding sources did not have any involvement in the study design; in the collection, analysis and interpretation of data; in the writing of the report; or in the decision to submit the article for publication.

Appendix A. Supplementary data

Supplementary data to this article can be found online at https://doi.

org/10.1016/j.biombioe.2021.106315.

References

[1] Biomass Explained, US Energy Inf. Adm, 2016. http://www.eia.gov/energyexplained/?page=biomass_home. (Accessed September 2021).

[2] O. Oyola-Rivera, A.M. González-Rosario, N. Cardona-Martínez, Catalytic production of sugars and lignin from agricultural residues using dilute sulfuric acid in γ-valerolactone, Biomass Bioenergy 119 (2018) 284–292, https://doi.org/10.1016/j.biombioe.2018.09.031.

[3] D.M. Alonso, J.Q. Bond, J.A. Dumesic, Catalytic conversion of biomass to biofuels, Green Chem. 12 (2010) 1493, https://doi.org/10.1039/c004654j.

[4] C.-H. Zhou, X. Xia, C.-X. Lin, D.-S. Tong, J. Beltramini, Catalytic conversion of lignocellulosic biomass to fine chemicals and fuels, Chem. Soc. Rev. 40 (2011) 5588, https://doi.org/10.1039/c1cs15124j.

[5] S.G. Wettstein, D.M. Alonso, E.I. Gürbüz, J.A. Dumesic, A roadmap for conversion of lignocellulosic biomass to chemicals and fuels, Curr. Opin. Chem. Eng. 1 (2012) 218–224, https://doi.org/10.1016/j.coche.2012.04.002.

[6] M.J. Climent, A. Corma, S. Iborra, Conversion of biomass platform molecules into fuel additives and liquid hydrocarbon fuels, Green Chem. 16 (2014) 516, https://doi.org/10.1039/c3gc41492b.

[7] F. Cao, T.J. Schwartz, D.J. McClelland, S.H. Krishna, J.A. Dumesic, G.W. Huber, Dehydration of cellulose to levoglucosenone using polar aprotic solvents, Energy Environ. Sci. 8 (2015) 1808–1815, https://doi.org/10.1039/C5EE00353A.

[8] P. Gallezot, Conversion of biomass to selected chemical products, Chem. Soc. Rev. 41 (2012) 1538–1558, https://doi.org/10.1039/C1CS15147A.

[9] R. Karinen, K. Vilonen, M. Niemelä, Biorefining: heterogeneously catalyzed reactions of carbohydrates for the production of furfural and hydroxymethylfurfural, ChemSusChem 4 (2011) 1002–1016, https://doi.org/10.1002/cssc.201000375.

[10] A.A. Rosatella, S.P. Simeonov, R.F.M. Frade, C.A.M. Afonso, 5-Hydroxymethylfurfural (HMF) as a building block platform: biological properties, synthesis and synthetic applications, Green Chem. 13 (2011) 754, https://doi.org/10.1039/c0gc00401d.

[11] B. Saha, M.M. Abu-Omar, Advances in 5-hydroxymethylfurfural production from biomass in biphasic solvents, Green Chem. 16 (2014) 24–38, https://doi.org/10.1039/C3GC41324A.

[12] R.-J. van Putten, J.C. van der Waal, E. de Jong, C.B. Rasrendra, H.J. Heeres, J.G. de Vries, Hydroxymethylfurfural, A versatile platform chemical made from renewable resources, Chem. Rev. 113 (2013) 1499–1597, https://doi.org/10.1021/cr300182k.

[13] Y.-C. Lin, J. Cho, G.A. Tompsett, P.R. Westmoreland, G.W. Huber, Kinetics and mechanism of cellulose pyrolysis, J. Phys. Chem. C 113 (2009), https://doi.org/10.1021/jp906702p, 20097–20107.

[14] Z. Wang, Q. Lu, X.-F. Zhu, Y. Zhang, Catalytic fast pyrolysis of cellulose to prepare levoglucosenone using sulfated zirconia, ChemSusChem 4 (2011) 79–84, https://doi.org/10.1002/cssc.201000210.

[15] N. Kuzhiyil, D. Dalluge, X. Bai, K.H. Kim, R.C. Brown, Pyrolytic sugars from cellulosic biomass, ChemSusChem 5 (2012) 2228–2236, https://doi.org/10.1002/cssc.201200341.

[16] X. Gong, Y. Yu, X. Gao, Y. Qiao, M. Xu, H. Wu, formation of anhydro-sugars in the primary volatiles and solid residues from cellulose fast pyrolysis in a wire-mesh reactor, Energy Fuels 28 (2014) 5204–5211, https://doi.org/10.1021/ef501112q.

[17] D. Reyes-Luyanda, J. Flores-Cruz, P.J. Morales-Pérez, L.G. Encarnación-Gómez, F. Shi, P.M. Voyles, N. Cardona-Martínez, Bifunctional materials for the catalytic conversion of cellulose into soluble renewable biorefinery feedstocks, Top. Catal. 55 (2012) 148–161, https://doi.org/10.1007/s11244-012-9791-5.

[18] Y.-S. Ooi, R. Zakaria, A. Rahman Mohamed, S. Bhatia, Hydrothermal stability and catalytic activity of mesoporous aluminum-containing SBA-15, Catal. Commun. 5 (2004) 441–445, https://doi.org/10.1016/j.catcom.2004.05.011.

[19] Y. Zhang, M. Flytzani-Stephanopoulos, Hydrothermal stability of cerium modified Cu-ZSM-5 catalyst for nitric oxide decomposition, J. Catal. 164 (1996) 131–145, https://doi.org/10.1006/jcat.1996.0369.

[20] D.W. Gardner, J. Huo, T.C. Hoff, R.L. Johnson, B.H. Shanks, J.-P. Tessonnier, Insights into the hydrothermal stability of ZSM-5 under relevant biomass conversion reaction conditions, ACS Catal. 5 (2015) 4418–4422, https://doi.org/10.1021/acscatal.5b00888.

[21] M.A. Mellmer, C. Sener, J.M.R. Gallo, J.S. Luterbacher, D.M. Alonso, J.A. Dumesic, Solvent effects in acid-catalyzed biomass conversion reactions, Angew. Chem. Int. Ed. 53 (2014) 11872–11875, https://doi.org/10.1002/anie.201408359.

[22] T.W. Walker, A.K. Chew, R.C. Van Lehn, J.A. Dumesic, G.W. Huber, Rational design of mixed solvent systems for acid-catalyzed biomass conversion processes using a combined experimental, molecular dynamics and machine learning approach, Top. Catal. (2020), https://doi.org/10.1007/s11244-020-01260-9.

[23] J. He, M. Liu, K. Huang, T.W. Walker, C.T. Maravelias, J.A. Dumesic, G.W. Huber, Production of levoglucosenone and 5-hydroxymethylfurfural from cellulose in polar aprotic solvent–water mixtures, Green Chem. 19 (2017) 3642–3653, https://doi.org/10.1039/C7GC01688C.

[24] M. Ostermeier, R. Schobert, Total synthesis of (+)-Chloriolide, J. Org. Chem. 79 (2014) 4038–4042, https://doi.org/10.1021/jo500527g.

[25] C. Müller, M.A. Gomez-Zurita Frau, D. Ballinari, S. Colombo, A. Bitto, E. Martegani, C. Airoldi, A.S. vanNeuren, M. Stein, J. Weiser, C. Battistini, F. Peri, Design, synthesis, and biological evaluation of levoglucosenone-derived Ras activation inhibitors, ChemMedChem 4 (2009) 524–528. https://doi.org/10.1002/cmdc.200800416.

[26] D.E. Richardson, W. Raverty, Predicted environmental effects from liquid emissions in the manufacture of levoglucosenone and Cyrene™, Appita J. 69 (2016) 344–351.

[27] B. Mended-Jorge, New flagship EU project focused on replacing toxic solvents with renewable alternatives. https://static1.squarespace.com/static/5643eb3de4b0c236a2510a8c/t/5e1544022bf7fe00a39baf48/1578451971796/v2+ReSolute+Press+Release+18+December+2019.pdf, 2019.

[28] O. Oyola-Rivera, J. He, G.W. Huber, J.A. Dumesic, N. Cardona-Martínez, Catalytic dehydration of levoglucosan to levoglucosenone using Brønsted solid acid catalysts in tetrahydrofuran, Green Chem. 21 (2019) 4988–4999, https://doi.org/10.1039/C9GC01526D.

[29] S. Kudo, X. Huang, S. Asano, J. Hayashi, Catalytic strategies for levoglucosenone production by pyrolysis of cellulose and lignocellulosic biomass, Energy Fuels 35 (2021) 9809–9824, https://doi.org/10.1021/acs.energyfuels.1c01062.

[30] S. Kudo, Z. Zhou, K. Norinaga, J. Hayashi, Efficient levoglucosenone production by catalytic pyrolysis of cellulose mixed with ionic liquid, Green Chem. 13 (2011) 3306, https://doi.org/10.1039/c1gc15975e.

[31] L. Qian, F. Xu, S. Liu, G. Lv, L. Jiang, T. Su, Y. Wang, Z. Zhao, Selective production of levoglucosenone by catalytic pyrolysis of cellulose mixed with magnetic solid acid, Cellulose 28 (2021) 7579–7592, https://doi.org/10.1007/s10570-021-04010-6.

[32] X. Huang, S. Kudo, S. Asano, J. Hayashi, Improvement of levoglucosenone selectivity in liquid phase conversion of cellulose-derived anhydrosugar over solid acid catalysts, Fuel Process. Technol. 212 (2021) 106625, https://doi.org/10.1016/j.fuproc.2020.106625.

[33] R. Yadav, T. Baskaran, A. Kaiprathu, M. Ahmed, S.V. Bhosale, S. Joseph, A.H. Al-Muhtaseb, G. Singh, A. Sakthivel, A. Vinu, Recent advances in the preparation and applications of organo-functionalized porous materials, Chem. Asian J. 15 (2020) 2588–2621, https://doi.org/10.1002/asia.202000651.

[34] D. Margolese, J.A. Malero, S.C. Christiansen, B.F. Chmelka, G.D. Stucky, Direct syntheses of ordered SBA-15 mesoporous silica containing sulfonic acid groups, Chem. Mater. 12 (2000) 2448–2459, https://doi.org/10.1021/cm0010304.

[35] J.A. Melero, R. van Grieken, G. Morales, Advances in the synthesis and catalytic applications of organosulfonic-functionalized mesostructured materials, Chem. Rev. 106 (2006) 3790–3812, https://doi.org/10.1021/cr050994h.

[36] A. Sayari, P. Liu, M. Kruk, M. Jaroniec, Characterization of large-pore MCM-41 molecular sieves obtained via hydrothermal restructuring, Chem. Mater. 9 (1997) 2499–2506, https://doi.org/10.1021/cm970128o.

[37] M. Kruk, M. Jaroniec, A. Sayari, Relations between pore structure parameters and their implications for characterization of MCM-41 using gas adsorption and X-ray diffraction, Chem. Mater. 11 (1999) 492–500, https://doi.org/10.1021/cm981006e.

[38] M. Kruk, M. Jaroniec, C.H. Ko, R. Ryoo, Characterization of the porous structure of SBA-15, Chem. Mater. 12 (2000) 1961–1968, https://doi.org/10.1021/cm000164e.

[39] M. Jaroniec, L.A. Solovyov, Improvement of the Kruk−Jaroniec−Sayari method for pore size analysis of ordered silicas with cylindrical mesopores, Langmuir 22 (2006) 6757–6760, https://doi.org/10.1021/la0609571.

[40] S.H. Krishna, T.W. Walker, J.A. Dumesic, G.W. Huber, Kinetics of levoglucosenone isomerization, ChemSusChem 10 (2017) 129–138, https://doi.org/10.1002/cssc.201601308.

[41] D.J.C. Constable, A.D. Curzons, V.L. Cunningham, Metrics to 'green' chemistry—which are the best? Green Chem. 4 (2002) 521–527, https://doi.org/10.1039/B206169B.

[42] R.A. Sheldon, Fundamentals of green chemistry: efficiency in reaction design, Chem. Soc. Rev. 41 (2012) 1437–1451, https://doi.org/10.1039/C1CS15219J.

[43] R.A. Sheldon, The E Factor: fifteen years on, Green Chem. 9 (2007) 1273, https://doi.org/10.1039/b713736m.

[44] G.R. Court, C.H. Lawrence, W.D. Reverty, A.J. Duncan, Method for Converting Lignocellulosic Materials into Useful Chemicals, US 2012/0111714 A1, 2012.

[45] W. Raverty, Levoglucosenone: à la recherche de chimie perdue, 2018. https://colloque.inrae.fr/explorebiomass/content/download/4041/41542/version/1/file/S5-Raverty.pdf. (Accessed September 2021).

[46] A. Galarneau, M. Nader, F. Guenneau, F. Di Renzo, A. Gedeon, Understanding the stability in water of mesoporous SBA-15 and MCM-41, J. Phys. Chem. C 111 (2007) 8268–8277, https://doi.org/10.1021/jp068526e.

[47] M.H. Tucker, A.J. Crisci, B.N. Wigington, N. Phadke, R. Alamillo, J. Zhang, S. L. Scott, J.A. Dumesic, Acid-functionalized SBA-15-type periodic mesoporous organosilicas and their use in the continuous production of 5-hydroxymethylfurfural, ACS Catal. 2 (2012) 1865–1876, https://doi.org/10.1021/cs300303v.